Pergamon

Scripta Materialia, Vol. 41, No. 3, pp. 289–296, 1999
Elsevier Science Ltd

1359-6462/99/$–see front matter

PII S1359-6462(99)00164-5

A MODIFIED ENERGY-BASED LOW CYCLE FATIGUE MODEL FOR EUTECTIC SOLDER ALLOY

X.Q. Shi, H.L.J. Pang*, W. Zhou*, and Z.P. Wang
Gintic Institute of Manufacturing Technology, Nanyang Drive, Singapore 638075
*School of Mechanical and Production Engineering, Nanyang Technological University, Nanyang Avenue, Singapore 639798

(Received April 21, 1999)
(Accepted May 7, 1999)

1. Introduction

Surface mount technology (SMT) is increasingly used in microelectronics to mount components by soldering onto the printed circuit board (PCB). The solder alloys are used as the electrical and mechanical connections between the component and the board. Fatigue failure of solder joints is recognized as a major cause of failure in electronic devices. An approach to this problem is to determine the fatigue behaviors of solder alloy by accelerated fatigue testing at different temperatures. In the present research, smooth specimens made entirely of a 63Sn/37Pb solder alloy were tested over a wide temperature range at various low frequencies to study its low cycle fatigue properties.

Strain-based models, notably the Coffin-Manson model (1–2), have been widely used to characterize low cycle fatigue behaviors of engineering materials including solder alloys (3–5). However, it is practically very difficult to obtain a single plastic strain value in a solder joint because of the complex stress state (6). In contrast, it is much easier to calculate energy density from the low cycle hysteresis loops for any types of solder joints under test (7). Therefore, in recent years, energy-based low cycle fatigue models have been increasingly used for solder alloys (7–9). These models are not so well established as the strain-based ones, and some researchers (10) even expressed doubt on whether energy density is a true parameter governing fatigue life of solder alloy. Therefore, in the study special effort was made to examine the existing energy-based models. In the end, a flow stress modified energy-based model is proposed based upon the examination and the experimental results. It is demonstrated in the paper that the new fatigue model can be used to predict the fatigue life of solder alloy at different frequencies or temperatures.

2. Experimental Procedures

The material used in the study was a eutectic alloy 63Sn/37Pb. This material is widely used as a solder in SMT. The chemical composition of the solder is as follows (in wt.%): 63.2 Sn, 0.006 Sb, 0.002 Cu, 0.004 Bi, 0.001 Zn, 0.002 Fe, 0.001 Al, 0.01 As, 0.001 Cd, and remainder Pb. Rods of the solder were produced by casting and then machined into cylindrical fatigue specimens of 90 mm long. The fatigue specimens have a diameter of 12 mm at the two ends and a central diameter of 6 mm with a radius of curvature of 105 mm in the gauge section to prevent any stress concentration due to sharp corners. After

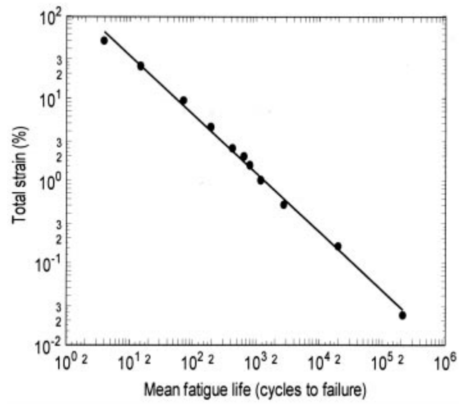

Figure 1. Strain-life data obtained at temperature 25 °C and frequency 1 Hz.

machining, the gauge section of each specimen was carefully ground on fine SiC paper and polished using 1 μm diamond paste. Afterwards, the fatigue specimens were annealed at 60 °C for 24 h in a N_2 atmosphere to eliminate the residual stresses.

The fatigue tests were conducted on a servo-valve-controlled electro-hydraulic testing machine newly designed by MTS (model 810). Gripping device of the machine was designed in such a way that only a small gripping load is required to grip the soft solder specimens. The machine has the capacity to produce very low frequencies in the wide range 10^{-4} to 1 Hz. The tests were run under a symmetrical uniaxial tension-compression loading with total strain control. During the testing, the crosshead was revised whenever half of the required total strain was attained. The strain was monitored using an extensometer attached to the gauge length of the fatigue specimen. The testing was carried out at five different frequencies (10^{-4}, 10^{-3}, 10^{-2}, 10^{-1} and 1 Hz) and at four different temperatures (25 °C, 75 °C, 125 °C and 150 °C) with total strain set at seven different values (0.5%, 1%, 2%, 5%, 10%, 25% and 50%).

3. Results and Discussion

For each test condition, six specimens were used. The number of cycles to failure for each of the specimens was recorded and the average value of the six readings was taken as the fatigue life. Generally, it is found that the fatigue life decreases with increasing total strain or decreasing frequency, as shown in Figs. 1–2. It is also observed that the fatigue life tends to decrease with increasing test temperature, but the temperature dependence is small. Figs. 1–2 serve to show representative results only, and other testing results will also be used to examine energy-based and strain-based models for the low cycle fatigue.

First, the Morrow energy model (11) was examined. The model predicts fatigue life (N_f) in terms of the plastic strain energy density (W_p), as shown below:

$$N_f^m W_p = C \tag{1}$$

where m is fatigue exponent, and C is material ductility coefficient. Typically, the hysteresis loop was observed to stabilize after a few cycles. The plastic strain energy density was determined from the area within the stable hysteresis loop. Fig. 3 shows fatigue life of the eutectic alloy as a function of strain energy density. The results in the figure were obtained at a fixed test temperature (25 °C) but at different frequencies (10^{-4} to 1 Hz) and different total strain levels (0.5% to 50%). The Morrow model predicts

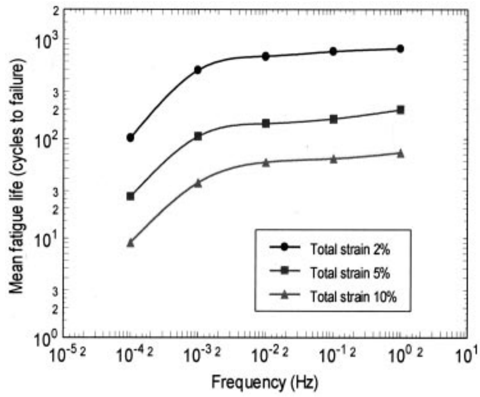

Figure 2. Life-frequency data obtained at temperature 25 °C.

a linear relationship between $log(N_f)$ and $log(W_p)$. When linear regression of $log(N_f)$ versus $log(W_p)$ was carried out using the results obtained at any given frequency, the Morrow energy model was found to describe the W_p–N_f relationship very well, as shown in Fig. 3. However, it should be noted that at any given strain energy density value the fatigue life strongly depends on the test frequency, indicating that it is not possible to use test results obtained at a certain frequency to predict fatigue life at a different frequency. The problem lies in that the "constants" (m and C) in the Morrow energy model actually change with test frequency, as can be seen clearly in Fig. 4. It is of interest to observe from Fig. 4 that for the eutectic solder studied the ductility coefficient (C) is more dependent on frequency than the fatigue exponent (m).

In order to account for the effect of frequency, a frequency-modified Coffin-Manson model (12) was then examined. The model predicts fatigue life (N_f) in terms of the plastic strain (ε_p), as shown below:

$$[N_f v^{(k-1)}]^m \varepsilon_p = C \tag{2}$$

where v is frequency, and k is a frequency exponent. The frequency exponent k can be determined from the relationship between fatigue life and frequency. As shown in Fig. 2, fatigue life of the solder studied is only slightly frequency-dependent in the frequency range 10^{-3} to 1 Hz but is strongly frequency-

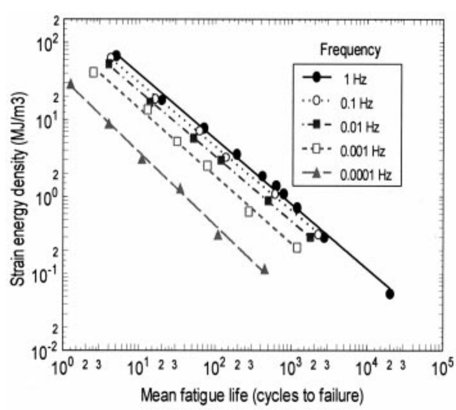

Figure 3. Relationship of fatigue life and strain energy density obtained at a fixed temperature (25 °C) but at different frequencies.

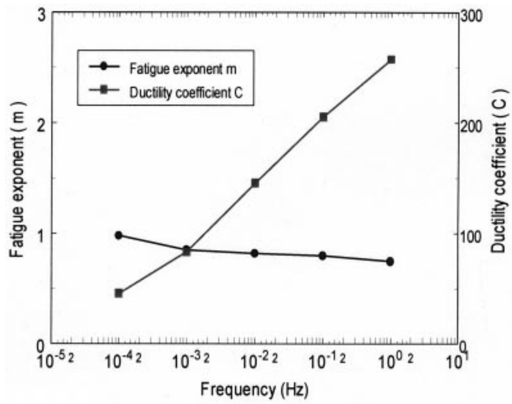

Figure 4. “Constants” in the Morrow energy model are shown using test results obtained at 25 °C, to depend on the test frequency.

dependent in the lower frequency range 10^{-4} to 10^{-3} Hz. Therefore, $(1 - k)$ value was calculated separately in the two frequency ranges and found to be 0.1 and 0.59 respectively. The $(1 - k)$ values were then used to calculate $N_f \nu^{(k-1)}$, which is the frequency-modified fatigue life. When the plastic strain is plotted against the frequency-modified fatigue life, the data points obtained at a wide range of frequencies (10^{-4} Hz to 1 Hz) were found to fit well into a single curve, as shown in Fig. 5. That is to say, the model can be used to eliminate the influence of frequency on the values of m and C. The experimental results in Fig. 5 were all obtained at a fixed temperature of 25 °C. Therefore, the question arises whether the values of m and C are independent of test temperature. It can be seen from Fig. 6 that the value of m is virtually independent of temperature but the value of C is still highly dependent on temperature. The temperature dependence of C was also reported by Solomon (3) for a slightly different solder alloy (60Sn/40Pb). To overcome the problem, Solomon averaged the C values over a temperature range. This approach obviously results in large errors in fatigue life.

Recently, Solomon and Tolksdorf (10) adopted a different approach by introducing a frequency-modified energy model, which incorporates both the frequency-modified strain energy density (W_p/ν^n) and the frequency modified fatigue life $(N_f \nu^{(k-1)})$, as shown below:

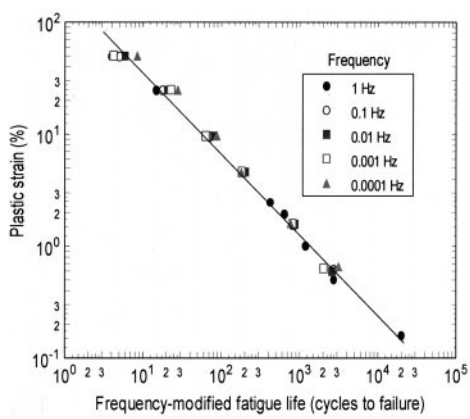

Figure 5. Relationship of frequency-modified fatigue life $(N_f \nu^{(k-1)})$ and plastic strain (ε_p) obtained at a fixed temperature (25 °C) but at different frequencies.

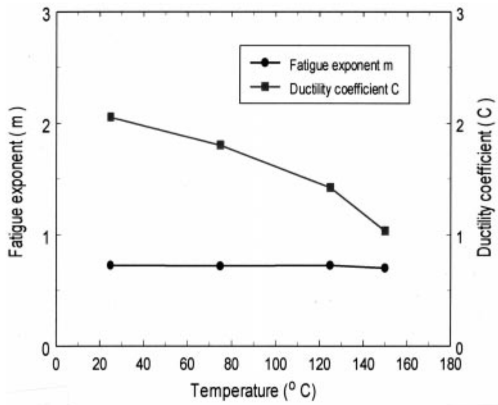

Figure 6. The value of C in the frequency-modified Coffin-Manson model is shown to be dependent on test temperature, although the value of m is almost a constant.

$$[N_f \nu^{(k-1)}]^m \frac{W_p}{\nu^n} = C \tag{3}$$

where k is a frequency exponent which is determined from the relationship between fatigue life and frequency as shown in Fig. 2, and n is another frequency exponent which is determined from the relationship between strain energy density and frequency (10). Unfortunately, the C value in this model is more dependent on temperature (it decreases from 250 to 5 as the temperature increases from −50 to 150 °C (10)) than that in the frequency-modified Coffin-Manson model.

Figs. 7–8 illustrate effect of frequency and temperature on hysteresis loops. At a certain total strain range and test temperature, the area within the hysteresis loop decreases with decreasing frequency (Fig. 7). At a certain total strain and frequency, the area of hysteresis loop decreases with increasing temperature (Fig. 8). This observation explains the dependence of fatigue life on frequency and temperature. Among the three models examined above, the Morrow energy-based model ignores the effect of frequency on fatigue life, so it is not surprising that it can not predict fatigue life at different frequencies. The other two models take into proper account the effect of frequency on fatigue life but

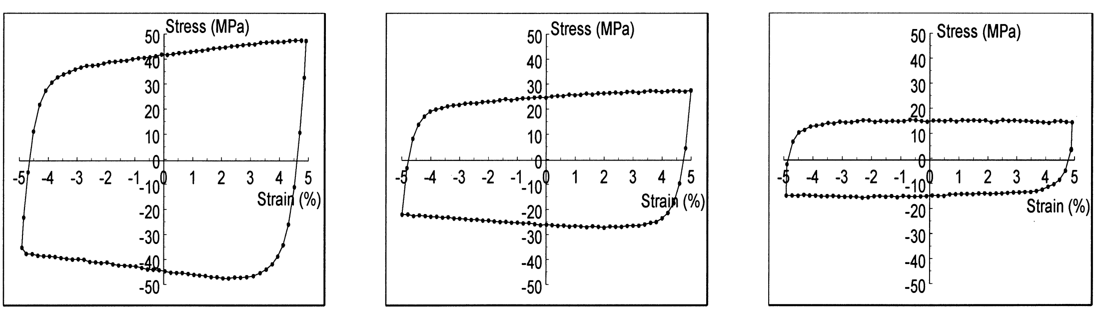

(a) 1 Hz (b) 10^{-2} Hz (c) 10^{-4} Hz

Figure 7. Hysteresis loops obtained at the same test temperature (25 °C) and the same strain range (10%) but at different frequencies of (a) 1 Hz, (b) 10^{-2} Hz, and (c) 10^{-4} Hz. The diagrams show that stress-strain relationship is significantly affected by frequency.

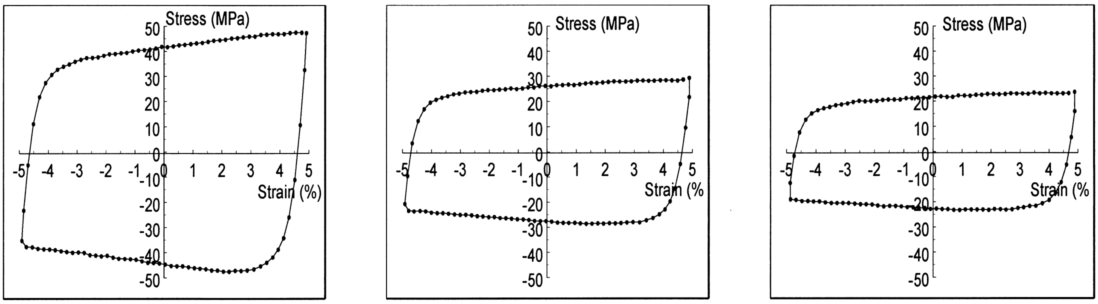

(a) 25 °C (b) 75 °C (c) 150 °C

Figure 8. Hysteresis loops obtained at the same frequency (1 Hz) and the same strain range (10%) but at different temperatures of (a) 2 °C, (b) 75 °C, and (c) 150 °C. The diagrams show that test temperature has pronounced effect on the stress-strain relationship.

do not account for the temperature influence, so the "constants" in the models are not independent of temperature.

Based on the above analysis, it can be argued that a temperature-dependent material parameter must be introduced into the frequency-modified energy model to reduce the temperature-dependence of the "constants." Therefore, a possible model should be of the following form:

$$[N_f \nu^{(k-1)}]^m \frac{W_p}{X} = C \tag{4}$$

where X is a certain temperature-dependent material parameter. When test temperature increases, the fatigue life N_f decreases and the area of hysteresis loop (thus W_p) also decreases (Fig. 8); according to Eq. (4), therefore, C would certainly decrease with increasing temperature if the parameter X were not introduced. To maintain the constancy of C, X must be a material parameter which decreases with increasing temperature. Fig. 8 shows clearly that flow stress of the material (σ_f) decreases with increasing temperature. Therefore, it is worthwhile to examine the following relationship:

$$[N_f \nu^{(k-1)}]^m \frac{W_p}{2\sigma_f} = C \tag{5}$$

The k value can be determined by the same method used in the frequency-modified energy-based model (10). The yield point and the highest point in the stress-strain curve within a hysteresis loop are taken and the values are averaged as the flow stress (σ_f). When the frequency-modified fatigue life ($N_f \nu^{(k-1)}$) is presented as a function of the flow stress-modified strain energy density ($W_p/2\sigma_f$), the data points obtained at a wide range of temperatures (25 to 150 °C) were found to fit well into a single curve, as shown in Fig. 9. That is to say, the parameter σ_f can be used to reduce effectively the influence of temperature on the value of C. As can be seen from Fig. 10, the constants in this model are not only frequency-independent but also relatively temperature independent. Therefore, the average values of m and C over the temperature range can be used to make a reasonable fit to all the experimental data. The average values of constants were found to be: $m = 0.70$, $C = 1.69$, $(1 - k) = 0.1$ for $\nu > 10^{-3}$ Hz or $(1 - k) = 0.59$ for $\nu < 10^{-3}$ Hz.

It is interesting to note from Eq. (5) that $W_p/2\sigma_f$ has the dimension of strain, so it may be referred to as "equivalent strain." The shape of hysteresis loops (Figs. 7–8) suggests that the equivalent strain is numerically close to the plastic strain ε_p; but the equivalent strain better reflects effect of temperature

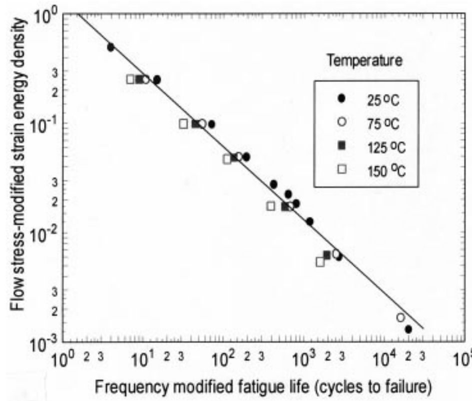

Figure 9. Relationship of frequency-modified fatigue life ($N_f \nu^{(k-1)}$) and flow stress-modified strain energy density ($W_p/2\sigma_f$).

on the mechanical behavior since it is a function of flow stress σ_f, which is highly dependent on temperature for the eutectic alloy. It should be noted that the eutectic alloy displayed visco-plastic behavior over the test temperature range. For the conventional materials with relatively temperature-independent flow stress, the new fatigue model proposed can be simplified as the strain-based Coffin-Manson model by changing the equivalent strain into the plastic strain, or the energy-based fatigue model by replacing the equivalent strain with the strain energy density. In other words, the conventional strain-based and energy-based fatigue models may be regarded as special cases of the new fatigue model.

4. Summary and Conclusions

Low cycle fatigue testing of a eutectic alloy 63Sn/37Pb was carried out over a wide range of frequencies (10^{-4} to 1 Hz) and temperatures (25 to 150 °C) with total strain set at different values (0.5% to 50%). The fatigue life was observed to decrease with decreasing frequency or increasing total strain, and it was also observed to decrease with increasing test temperature although the temperature dependence was relatively small. The Morrow energy-based model, the frequency-modified Coffin-Manson model, and

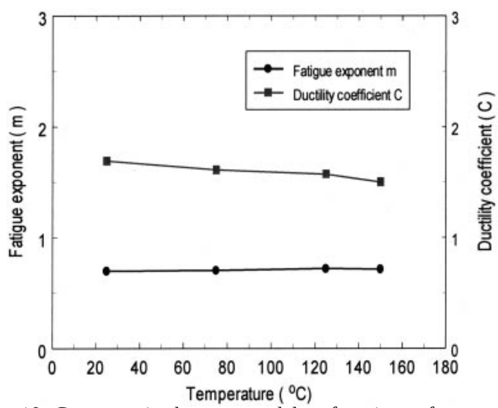

Figure 10. Constants in the new model as functions of temperature.

the frequency-modified energy-based model by Solomon were examined in the study. It was found that the Morrow model can not predict the fatigue life at different frequencies because it ignores the effect of frequency on fatigue life. The other two models take into proper account the effect of frequency on fatigue life but do not account for the temperature influence, so the “constants” in the models are not independent of temperature. Flow behavior of the eutectic solder was observed to be visco-plastic and strongly dependent on temperature; therefore, flow stress was introduced into the frequency-modified energy model to account for influence of temperature on the fatigue life. The new fatigue model was found to be able to predict the fatigue life at different frequencies or temperatures. It would be interesting to study further whether the new model could be applied to other visco-plastic materials.

References

1. L. F. Coffin, Jr., ASME Trans. 76, 931 (1954).
2. S. S. Manson, Exp. Mech. 5, 193 (1965).
3. H. D. Solomon, IEEE Trans. Compon. Hybrids Manuf. Technol. 9, 423 (1986).
4. Q. Guo, E. C. Cutiongco, M. E. Fine, and L. Keer, ASME J. Electron. Packaging. 114, 145 (1992).
5. N. F. Enke, T. J. Kilinsli, S. A. Schroeder, and J. R. Lesniak, IEEE Trans. CHMT. 12, 459 (1989).
6. B. Z. Hong, T. D. Yuan, and L. Burrell, ASME Sensing Modeling Simulation Emerging Electron. Packaging. 17, 39 (1996).
7. A. Dasgupta, C. Oyan, D. Barker, and M. Pecht, ASME J. Electron. Packaging. 114, 152 (1992).
8. W. Engelmaier and A. I. Attarawala, IEEE Trans. CHMT. 12, 284 (1989).
9. H. D. Solomon and E. D. Tolksdorf, ASME J. Electron. Packaging. 118, 67 (1996).
10. H. D. Solomon and E. D. Tolksdorf, ASME J. Electron. Packaging. 117, 130 (1995).
11. J. D. Morrow, ASTM STP 378, p. 45, ASTM, Philadelphia (1964).
12. L. F. Coffin, Jr., ASTM STP 520, p. 5, ASTM, Philadelphia (1973).